

# Silicate rock weathering and atmospheric/soil CO<sub>2</sub> uptake in the Amazon basin estimated from river water geochemistry: seasonal and spatial variations

Jefferson Mortatti<sup>a</sup>, Jean-Luc Probst<sup>b,\*</sup>

<sup>a</sup>*Centro de Energia Nuclear na Agricultura, CENA/USP, Av. Centenário, 303, CP 96, CEP: 13416-000, Piracicaba, São Paulo, Brazil*

<sup>b</sup>*Laboratoire des Mécanismes de Transfert en Géologie, UMR CNRS/Université Paul Sabatier 5563, 38 rue des 36 ponts, 31400 Toulouse, France*

---

## Abstract

Using the data of the CAMREX project (1982–1984) on the water geochemistry of the Amazon river and its main tributaries, it was possible to assess the silicate rock weathering processes and the associated consumption of atmospheric/soil CO<sub>2</sub>, taking into account seasonal and spatial variations. This study confirms the important role of the Andes in the fluvial transport of dissolved and particulate material by the Amazon, and it shows for the first time that the silicate weathering rate and atmospheric/soil CO<sub>2</sub> consumption are higher in the Andes than in the rest of the Amazon basin.

The seasonal variations exhibit the significant role of runoff as a major factor controlling silicate weathering processes and show that the chemical erosion rates vary greatly from low discharge to high discharge. The average weathering rate estimated for the whole Amazon basin (15 m/My) is comparable to other estimations made for other tropical–equatorial environments. A comparison between physical and chemical weathering rates of silicate rocks for the Amazon basin and for each tributary basin show that in the Andes and in the Amazon trough, the soil thicknesses are decreasing whereas in the Shield the soil profiles are deepening.

*Keywords:* Riverine transport; Physical erosion; Chemical weathering; Atmospheric/soil CO<sub>2</sub>; Amazon basin

---

## 1. Introduction

The riverine transport of dissolved and particulate materials to the oceans is generally related to a large

number of interactions involving climatic, hydrological, physico-chemical and biological aspects. The mechanical erosion process, basically related to the particulate river transport, tends to promote a reduction of the soil thickness. Whereas chemical erosion, related to the dissolved river transport, tends to a deepening of the soil weathering profile. In other words, mechanical erosion is related to soil loss, while chemical erosion could be associated with soil for-

---

\* Corresponding author. Tel.: +33-5-61556162; fax: +33-5-61520544.

*E-mail addresses:* [jmortatt@cena.usp.br](mailto:jmortatt@cena.usp.br) (J. Mortatti), [jlprobst@cict.fr](mailto:jlprobst@cict.fr) (J.-L. Probst).

mation. Consequently, a soil equilibrium approach must consider both processes (Probst, 1992; Gaillardet et al., 1997; Boeglin and Probst, 1998).

The chemical erosion of inorganic materials, which consists of dissolving or hydrolyzing primary minerals of rocks and soils, requires CO<sub>2</sub> and produces alkalinity. The flux of CO<sub>2</sub> consumed by weathering processes is mainly produced by oxidation of soil organic matter. Nevertheless, on a geological time scale, the flux of CO<sub>2</sub> consumed by carbonate dissolution on the continents is balanced by the CO<sub>2</sub> flux released to the atmosphere by carbonate precipitation in the oceans. Consequently, with regard to the global carbon cycle and particularly to the CO<sub>2</sub> content in the atmosphere, it is only the fluxes of CO<sub>2</sub> consumed by silicate rock weathering which represent a net sink of CO<sub>2</sub> and which is naturally equilibrated by CO<sub>2</sub> release from volcanism and metamorphism processes.

Since the last decades, several researchers tried to explain the variations of the Earth surface temperature during the geological times. Walker et al. (1981) and Berner et al. (1983) have proposed that the temperature is controlled on a global scale by a feedback mechanism between the atmospheric CO<sub>2</sub> and the silicate rock weathering. This mechanism has been used in different models to reconstruct the CO<sub>2</sub> content in the atmosphere during the geological times (Berner, 1994; Berner and Kothavala, 2001; François and Walker, 1992; Godd eris and Fran ois, 1995; Wallmann, 2001). Raymo and Ruddimann (1992) and Edmond (1992) made also the hypothesis that the formation of mountains could play a major role in the Earth climate evolution. This hypothesis is based on the idea that mechanical erosion of rocks increases the reactive surface of the minerals with water and, finally, increases their chemical weathering rates (Stallard and Edmond, 1981; Gaillardet et al., 1995) and consequently the associated CO<sub>2</sub> consumption. Recent works have shown that there is a good relationship between mechanical erosion and chemical weathering for large river basins (Gaillardet et al., 1999a) as well as for small rivers (Millot et al., 2002), strengthening also the major role of the mountains on the CO<sub>2</sub> content in the atmosphere.

Since the last 10 years, several studies on weathering processes have been also focused on silicate rocks to determine the major factors (temperature,

precipitation, runoff, lithology) controlling their weathering rates (White and Blum, 1995; Gislason et al., 1996; Gaillardet et al., 1999a,b; Dessert et al., 2001; Millot et al., 2002).

The Amazon river and its tributaries drain the largest river basin of the world ( $4.6 \times 10^6$  km<sup>2</sup> at  bidos) and the Amazon discharge at  bidos (160 000 m<sup>3</sup> s<sup>-1</sup> on average for the 20th century) is the highest in the world. The contribution of the Amazon river to the global riverine fluxes of dissolved and suspended materials to the oceans represents, respectively, 6% and 8–10%. Moreover, in the Amazon basin, silicate rocks occupy 96% of the total drainage area (Amiotte Suchet, 1995; Amiotte Suchet et al., in press) and, consequently, the contribution of the Amazon basin to the global CO<sub>2</sub> uptake by silicate rock weathering is very significant (5–15% according to the estimations: Amiotte Suchet, 1995; Amiotte Suchet et al., in press). Most of the studies (Gibbs, 1967; Stallard, 1980; Stallard and Edmond, 1983; Tardy et al., 1993a,b; Amiotte Suchet and Probst, 1993b; Probst et al., 1994; Gaillardet et al., 1997; Mortatti et al., 1997) devoted to the Amazon river transports and to the chemical erosion have not been focused on silicate weathering and no study has looked at the seasonal variations.

The main objective of this paper is to focus the study on the silicate weathering processes using the data of the Carbon in the AMazon River EXperiment (CAMREX) project (Richey and Salati, 1985; Richey et al., 1986, 1989, 1990, 1991) on major dissolved elements transported by the Amazon river and its main tributaries. The CAMREX was a cooperative research project of the University of Washington (Seattle, WA, USA), the Instituto Nacional de Pesquisas da Amazonia (Manaus, Brazil) and the Centro de Energia Nuclear na Agricultura (Piracicaba, Brazil). The objective of the CAMREX project was to study the distributions and dynamics of water flow, sediment and nutrients in the Amazon main channel.

The main scientific questions that this paper tries to answer using the CAMREX data are the following:

- What is the soil equilibrium, i.e. physical erosion versus chemical weathering, in the different morphostructural regions of the Amazon (the Andes, the Shield and the Amazon trough)?

- Is the silicate rock weathering and the associated CO<sub>2</sub> uptake more important in the Andes than in the rest of the Amazon basin?
- What are the seasonal variations of silicate weathering rate and CO<sub>2</sub> uptake in the different Amazonian regions?

## 2. Hydrological and geological characteristics of the Amazon river basin

The Amazon basin, located mainly in the equatorial belt, drains an area of 4 619 000 km<sup>2</sup> at Óbidos station (Brasil, 1987). The mean annual precipitation is variable from 1500 to 3000 mm, according to the station. It has been estimated that about 50% of the rainfall returns to the atmosphere by evapotranspiration and the rest discharges into the ocean (Salati, 1985).

The discharge of the Amazon is greatly variable according to the season and according to the year. The monthly discharge data for the Amazon at Óbidos station indicate that for the period 1902–1998, the maximum and minimum monthly value occur, respectively, in June (219 000 m<sup>3</sup> s<sup>-1</sup>) and in November (104 000 m<sup>3</sup> s<sup>-1</sup>), showing that the ratio between high and low waters averages 2.1. For the same period, the maximum and minimum mean annual discharge was respectively observed in 1993–1994 (192 000 m<sup>3</sup> s<sup>-1</sup>) and in 1925–1926 (112 000 m<sup>3</sup> s<sup>-1</sup>). Notwithstanding the spatial variation of precipitation over the whole basin, the Amazon river shows a remarkable regularity in discharge during the different seasons (high waters from May to August and low waters from September to December).

The hydrological characteristics of the Amazon river can be summarized as a mixing of three major hydrological regimes: equatorial and tropical regimes

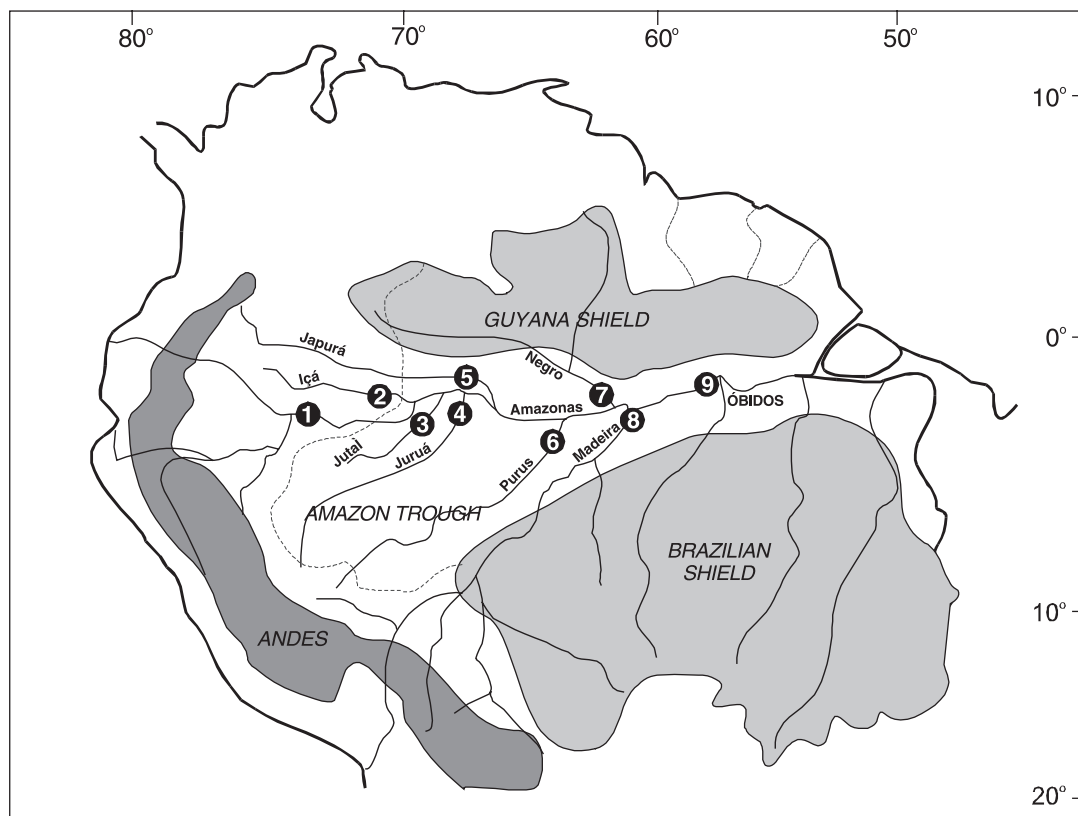


Fig. 1. Morphostructural zones, main tributaries and sampling points of the Amazon basin. 1—Solimões river at Vargem Grande (drainage basin area: 1 134 540 km<sup>2</sup>); 2—Içá (148 000 km<sup>2</sup>); 3—Jutai (74 000 km<sup>2</sup>); 4—Juruá (217 000 km<sup>2</sup>); 5—Japurá (289 000 km<sup>2</sup>); 6—Purus (372 000 km<sup>2</sup>); 7—Negro (755 000 km<sup>2</sup>); 8—Madeira (1 380 000 km<sup>2</sup>); 9—Amazon river at Óbidos (4 619 000 km<sup>2</sup>).

in the North and in the South concerning, respectively, the left and right side tributaries and snowmelting regimes in the East, near the Andes Mountain. The important contributions of two main tributaries can be noted: Madeira and Negro rivers are responsible for 16 and 18%, respectively, of the total runoff at Óbidos (Mortatti, 1995). The upper Solimões river drains about 65% of the Andean part of the Amazon basin while the upper Madeira river drains 35% of the total basin area (Fig. 1). The total water volume discharged by the Amazon river to the ocean is estimated at  $5.0 \times 10^3 \text{ km}^3/\text{year}$ , roughly 15% of the total global runoff. The Amazon river in South America and the Congo river in Africa, together, are responsible for about 60% of the total fresh water input to the Atlantic Ocean (Probst et al., 1994).

The drainage basin of the Amazon river is characterized by a diversity of geological formations, distributed in three major morphostructural zones (Stallard and Edmond, 1983): (i) the Precambrian Shields with metamorphic and igneous rocks; (ii) the Andean Cordillera with carbonate rocks and

evaporites; and (iii) the Amazon Trough with Tertiary sediments and Pleistocene fluvial deposits. The northern tributaries drain the Guyana Shield and part of the sub-Andean region. The southern tributaries drain part of the Brazilian Shield and part of the Bolivian and Peruvian Andean Cordillera (Fig. 1).

The difference between the lithological distribution of this region is responsible for the difference of water quality observed in the basin. The surface water chemistry and the dissolved and particulate river transports are strongly influenced by the geology, as shown by Stallard and Edmond (1983), but also take into account the influence of the atmospheric inputs by precipitation (Gibbs, 1967; Stallard and Edmond, 1981). As mentioned previously, the Amazon basin is dominated by silicate terrains that occupy 96.1% of the total area. In detail, the contribution of each main lithology is the following: 16.7% of sands and sandstones, 50.7% of shales, 26.8% of plutonic and metamorphic rocks, 1.9% of volcanic acid rocks and 3.9% of carbonate rocks (Amiotte Suchet et al., in press).

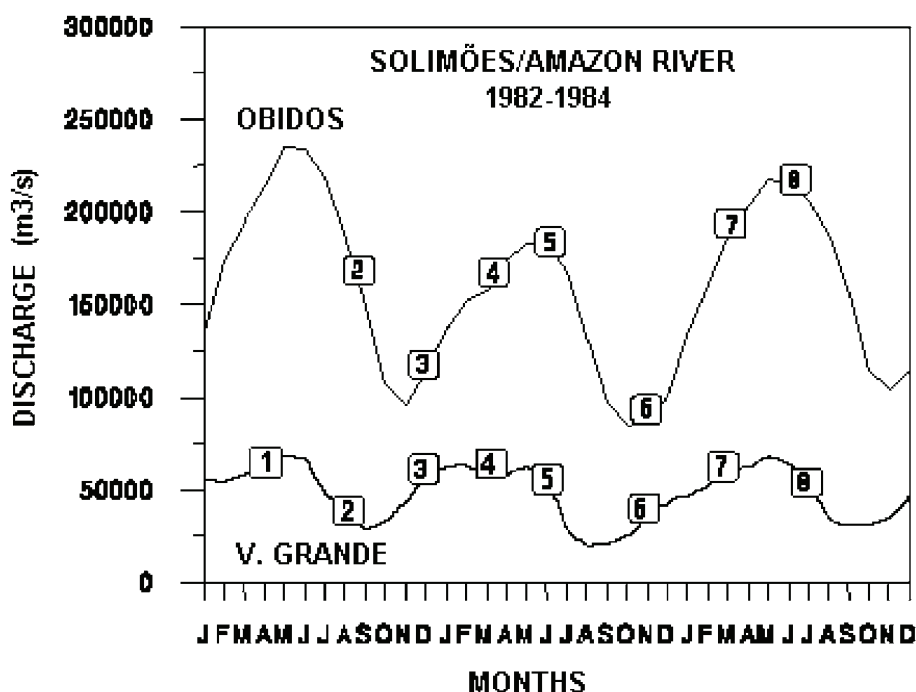


Fig. 2. Solimões/Amazon river discharge variations at Vargem Grande and Óbidos sampling stations during the CAMREX cruises: 1 (April–May 1982), 2 (August–September 1982), 3 (November–December 1982), 4 (March–April 1983) 5 (June–July 1983), 6 (October–November 1983), 7 (February–March 1984) and 8 (July–August 1984).

### 3. Solute river transport and chemical erosion

The solute transport of the Amazon river main-stream and major tributaries have been estimated by Mortatti (1995) from the average values of the dissolved load obtained during the eight cruises (Fig. 2) of the CAMREX project (1982–1984) and reported in the literature (Richey et al., 1986, 1989, 1990; Devol et al., 1987; Martinelli et al., 1989). Some original data for  $\text{SO}_4^{2-}$  concentrations were corrected when the ionic balance of the solution was not equilibrated, taking into account the spatial and temporal variations of their concentrations in relation to the river discharge (see Mortatti et al., 1997). Table 1 shows the concentrations of the major chemical species for the Amazon rivers during the low and high river water stages. The average values are weighted by the respective discharges as determined from eight cruises along the Amazon main-stream and tributaries. The concentrations of the major anions (see Fig. 3 for  $\text{HCO}_3^-$ ) and cations (see Fig. 4 for  $\text{Ca}^{2+}$ ) are greatly variable from one

station to another but also for the same station, from one cruise to another. The rivers draining the shield (Negro) and the Amazon trough (Jutai, Içã, Japurá) present the lowest concentrations ( $1-10^2 \mu\text{M l}^{-1}$ ), whereas the rivers draining the Andes (Solimões, Madeira, Juruá, Purus) and the Amazon at Óbidos have the highest concentrations ( $10-10^3 \mu\text{M l}^{-1}$ ). When comparing the concentrations (Figs. 3 and 4) with the chemical compositions (Fig. 5), it appears that the more concentrated waters are mainly composed of bicarbonate ions and calcium, whereas the chemical composition of dilute waters tends to chloride and sodium poles. The respective contribution of magnesium and sulfate to the cationic and anionic charge is very low (20% maximum). The contribution of potassium to the cationic charge does not exceed 30%.

Among the chemical species transported by the Amazon river to the ocean,  $\text{HCO}_3^-$ ,  $\text{SiO}_2$  and  $\text{Ca}^{2+}$  exhibit the most important annual fluxes with  $131.5 \times 10^6$ ,  $38.1 \times 10^6$  and  $33.9 \times 10^6$  tons, respectively. The contributions of each tributary to the

Table 1  
Concentrations (in  $\mu\text{M l}^{-1}$ ) of the major chemical species for the Amazon river and its main tributaries during the low and high river water stages

| Cations  | Ca  |      |         | Mg  |      |         | Na  |      |         | K   |      |         |
|----------|-----|------|---------|-----|------|---------|-----|------|---------|-----|------|---------|
|          | Low | High | Average | Low | High | Average | Low | High | Average | Low | High | Average |
| (1) VGr  | 374 | 413  | 457     | 77  | 78   | 80      | 241 | 217  | 218     | 26  | 31   | 32      |
| (2) RIça | 32  | 35   | 35      | 13  | 17   | 14      | 37  | 43   | 44      | 7   | 12   | 13      |
| (3) RJut | 17  | 53   | 59      | 8   | 2    | 11      | 62  | 30   | 46      | 15  | 16   | 16      |
| (4) RJur | 497 | 231  | 257     | 70  | 59   | 60      | 261 | 137  | 123     | 39  | 32   | 33      |
| (5) RJap | 33  | 27   | 48      | 11  | 12   | 14      | 53  | 44   | 56      | 13  | 10   | 12      |
| (6) RPur | 157 | 93   | 84      | 56  | 31   | 28      | 173 | 80   | 69      | 30  | 25   | 26      |
| (7) RNeg | 7   | 9    | 9       | 4   | 6    | 5       | 52  | 54   | 39      | 6   | 13   | 11      |
| (8) RMad | 200 | 120  | 133     | 107 | 76   | 79      | 253 | 100  | 95      | 30  | 35   | 38      |
| (9) OBi  | 178 | 140  | 171     | 47  | 39   | 47      | 183 | 109  | 107     | 20  | 23   | 26      |

| Anions and $\text{SiO}_2$ | $\text{HCO}_3^-$ |      |         | Cl  |      |         | $\text{SO}_4$ |      |         | $\text{SiO}_2$ |      |         |
|---------------------------|------------------|------|---------|-----|------|---------|---------------|------|---------|----------------|------|---------|
|                           | Low              | High | Average | Low | High | Average | Low           | High | Average | Low            | High | Average |
| (1) VGr                   | 850              | 910  | 988     | 188 | 130  | 128     | 73            | 80   | 87      | 183            | 166  | 162     |
| (2) RIça                  | 119              | 83   | 100     | 3   | 45   | 33      | 1             | 8    | 5       | 111            | 107  | 109     |
| (3) RJut                  | 85               | 60   | 61      | 11  | 28   | 52      | 3             | 8    | 16      | 156            | 134  | 131     |
| (4) RJur                  | 1000             | 566  | 632     | 200 | 50   | 56      | 50            | 15   | 14      | 204            | 184  | 184     |
| (5) RJap                  | 95               | 94   | 128     | 28  | 17   | 25      | 7             | 4    | 6       | 104            | 87   | 95      |
| (6) RPur                  | 565              | 278  | 266     | 34  | 22   | 24      | 3             | 7    | 7       | 202            | 150  | 160     |
| (7) RNeg                  | 24               | 30   | 18      | 14  | 16   | 18      | 3             | 4    | 4       | 73             | 70   | 66      |
| (8) RMad                  | 550              | 374  | 378     | 81  | 22   | 27      | 130           | 51   | 56      | 135            | 142  | 141     |
| (9) OBi                   | 423              | 387  | 435     | 80  | 41   | 51      | 35            | 14   | 32      | 137            | 120  | 128     |

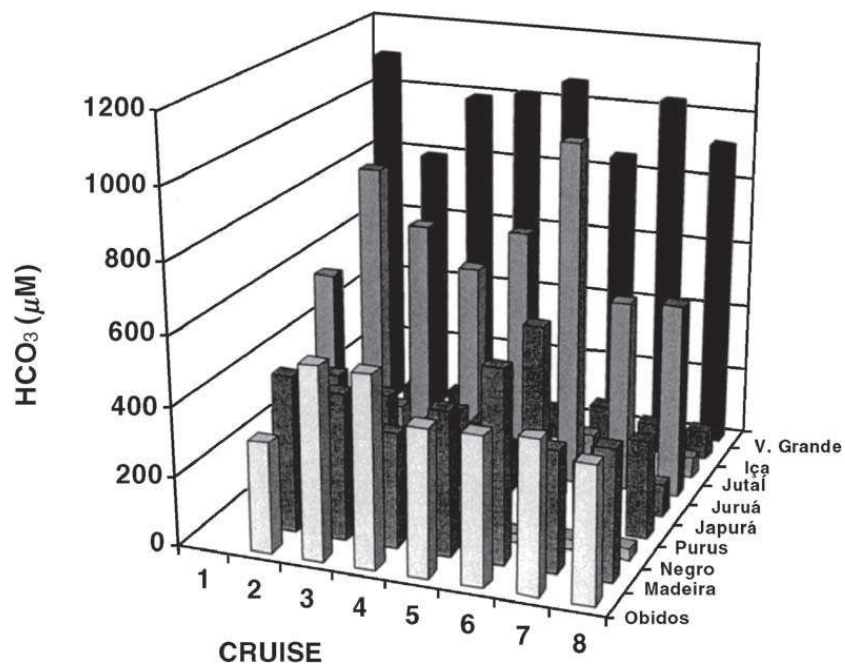


Fig. 3. Distribution of bicarbonate concentrations  $\mu\text{M l}^{-1}$  along the Solimões/Amazon river and main tributaries during the eight CAMREX cruises of the period 1982–1984.

dissolved load transported by the Amazon river to the ocean are reported in Table 2. It can be noted the influence of the carbonate rock dissolution in the

upper part of the basin (station 1, Vargem Grande, see Fig. 1), where the  $\text{HCO}_3^-$  river transport is very important.

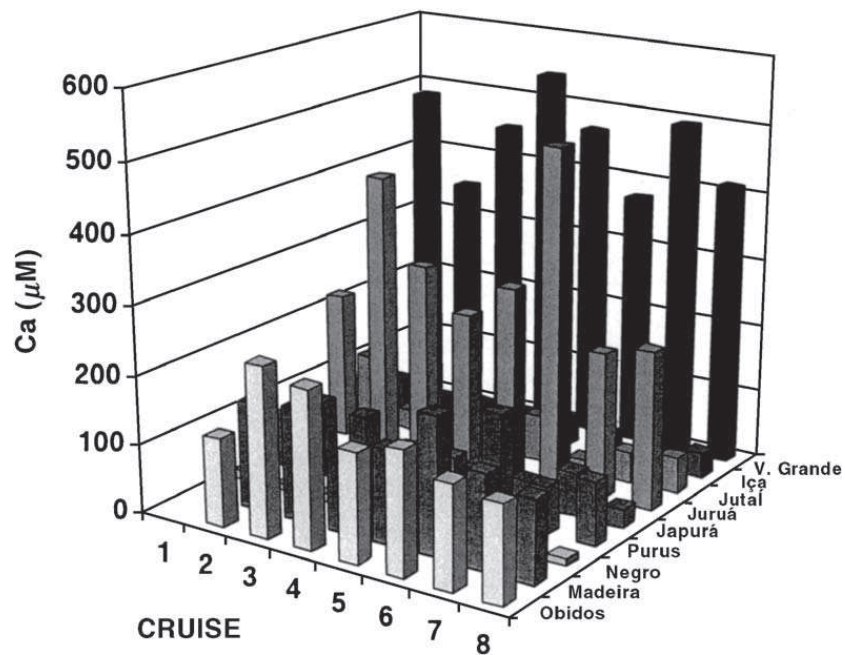


Fig. 4. Distribution of calcium concentrations  $\mu\text{M l}^{-1}$  along the Solimões/Amazon river and main tributaries during the eight CAMREX cruises of the period 1982–1984.

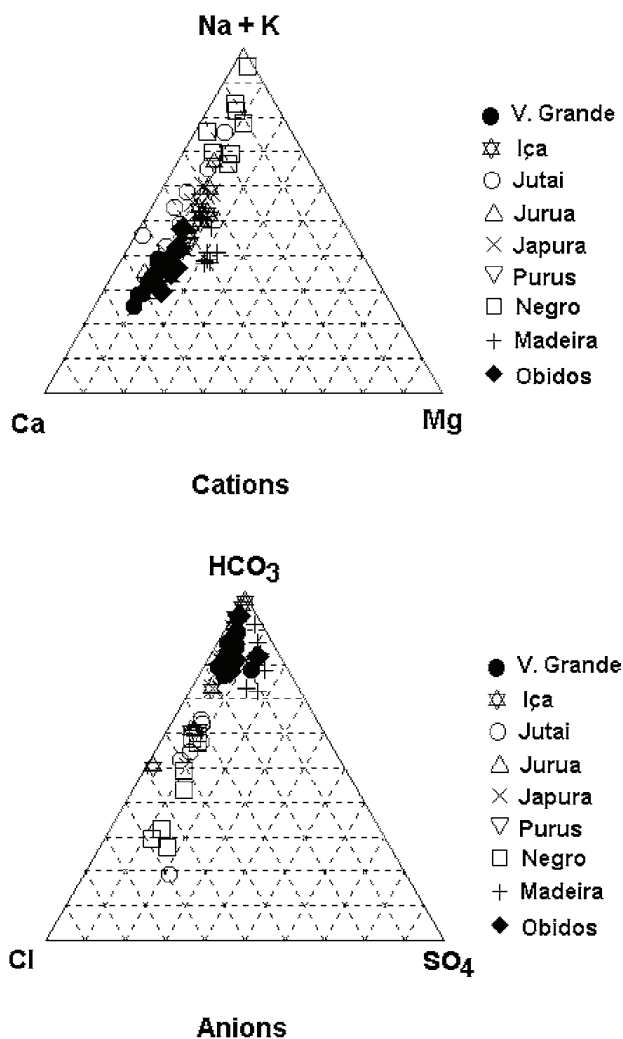


Fig. 5. Cationic (above) and anionic (below) chemical compositions of the different river waters (Solimões at Vargem Grande, Amazon at Óbidos, main tributaries) draining the Amazon basin during the period 1982–1984. Each point represents the chemical composition of a river water sample collected during each CAMREX cruise.

The calculated mean value for the total dissolved solids (TDS = cations + anions + silica) carried out to the ocean is estimated to be  $250.6 \times 10^6$  tons/year, of which about 80% originate from the Andes, which includes the Solimões ( $162.1 \times 10^6$  tons/year) and the Madeira ( $39.2 \times 10^6$  tons/year) river contributions. The remaining 20% is supplied by the rivers which drains the shield (Negro:  $7.2 \times 10^6$  tons/year) and the Amazon trough (Iça, Jutai, Juruá, Japurá and Purus: respectively 4, 2.1, 8.1, 9.5 and  $12.9 \times 10^6$  tons/year). During the low water stage, the TDS transport is

approximately 65% of the mean value, in spite of higher concentrations of the chemical species.

The black waters, such as the Negro river water from the Guyana shield, are very dilute, explaining its very small contribution (smaller than 3.0%) to the total dissolved load of the Amazon river.

If one compares the mean Amazon dissolved load with some other major world rivers, one can observe that the total dissolved river transport (in tons) is higher for the Amazon than for the Ganges–Bramaputra ( $134.8 \times 10^6$  tons/year according to Meybeck, 1979) and for the Yangtze ( $167.7 \times 10^6$  tons/year according to Wei-Bin, 1985) rivers, due to higher mean discharge values, while the specific dissolved loads (in tons/km<sup>2</sup>) are lower due to larger drainage basin area and to lower carbonate rock abundance according to the data of Amiotte Suchet et al. (in press) (3.9% in the Amazon basin, 33.8% in the Ganges–Bramaputra and 44% in the Yangtze river).

According to Mortatti (1995), the relationships between the concentration of the major dissolved elements and the river discharge for the lower Amazon show decreasing patterns, similar to theoretical dilution curves defined by Probst (1992) as the dilution of the highest concentration measured during low water period by increasing water discharge with a constant concentration close to zero, except for potassium, which is greatly involved in the biological cycles. In the upper basin, Ca<sup>2+</sup>, K<sup>+</sup> and HCO<sub>3</sub><sup>-</sup> concentrations, increase with the discharge, showing superficial origins as already pointed out by Probst et al. (1994). This means that these elements are stored in the soils and washed out during the high water periods. On the contrary, Cl<sup>-</sup>, SO<sub>4</sub><sup>2-</sup> and Na<sup>+</sup> follow the theoretical dilution curves.

#### 4. Correction for atmospheric inputs

In order to determine the origins of the major element fluxes transported by the Amazon river and to calculate the chemical erosion rate in the basin, it was necessary to determine first the contribution of the atmospheric inputs (ions and CO<sub>2</sub>) to the total river loads and to correct the river transport for these atmospheric inputs.

For the Amazon basin, the chemistry of the precipitation was investigated previously by Stallard and

Table 2

Transport of the major chemical species (in  $10^6$  tons/year) by the Amazon river and its main tributaries during low and high river water periods

| Flux ( $\times 10^6$ tons/year) | Ca   |      |         | Mg  |      |         | Na   |      |         | K   |      |         |
|---------------------------------|------|------|---------|-----|------|---------|------|------|---------|-----|------|---------|
|                                 | Low  | High | Average | Low | High | Average | Low  | High | Average | Low | High | Average |
| (1) VGr                         | 12.5 | 25.0 | 27.1    | 1.6 | 2.9  | 2.9     | 4.6  | 7.6  | 7.4     | 0.9 | 1.8  | 1.9     |
| (2) RIça                        | 0.2  | 0.4  | 0.3     | 0.1 | 0.1  | 0.1     | 0.2  | 0.3  | 0.2     | 0.1 | 0.1  | 0.1     |
| (3) RJut                        | 0.0  | 0.2  | 0.3     | 0.0 | 0.0  | 0.0     | 0.1  | 0.1  | 0.1     | 0.0 | 0.1  | 0.1     |
| (4) RJur                        | 0.6  | 1.4  | 1.2     | 0.0 | 0.2  | 0.2     | 0.2  | 0.5  | 0.3     | 0.0 | 0.2  | 0.2     |
| (5) RJap                        | 0.6  | 0.6  | 1.0     | 0.1 | 0.2  | 0.2     | 0.6  | 0.5  | 0.6     | 0.2 | 0.2  | 0.2     |
| (6) RPur                        | 0.6  | 1.9  | 1.3     | 0.1 | 0.4  | 0.3     | 0.4  | 0.9  | 0.6     | 0.1 | 0.5  | 0.4     |
| (7) RNeg                        | 0.1  | 0.5  | 0.3     | 0.0 | 0.2  | 0.1     | 0.5  | 1.8  | 0.8     | 0.1 | 0.7  | 0.4     |
| (8) RMad                        | 1.7  | 2.9  | 4.3     | 0.6 | 1.1  | 1.5     | 1.2  | 1.4  | 1.8     | 0.3 | 0.8  | 1.2     |
| (9) OBi                         | 20.6 | 35.9 | 33.9    | 3.3 | 6.1  | 5.7     | 12.2 | 16.0 | 12.2    | 2.3 | 5.8  | 5.0     |

| Flux ( $\times 10^6$ tons/year) | HCO <sub>3</sub> |       |         | Cl  |      |         | SO <sub>4</sub> |      |         | SiO <sub>2</sub> |      |         |
|---------------------------------|------------------|-------|---------|-----|------|---------|-----------------|------|---------|------------------|------|---------|
|                                 | Low              | High  | Average | Low | High | Average | Low             | High | Average | Low              | High | Average |
| (1) VGr                         | 43.5             | 84.0  | 89.3    | 5.6 | 7.0  | 6.7     | 5.9             | 11.6 | 12.4    | 9.2              | 15.1 | 14.4    |
| (2) RIça                        | 1.3              | 1.3   | 1.4     | 0.0 | 0.4  | 0.3     | 0.0             | 0.2  | 0.1     | 1.2              | 1.7  | 1.5     |
| (3) RJut                        | 0.2              | 0.4   | 0.4     | 0.0 | 0.1  | 0.2     | 0.0             | 0.1  | 0.2     | 0.4              | 0.8  | 0.8     |
| (4) RJur                        | 1.7              | 5.2   | 4.5     | 0.2 | 0.3  | 0.2     | 0.1             | 0.2  | 0.2     | 0.3              | 1.7  | 1.3     |
| (5) RJap                        | 2.7              | 3.0   | 3.9     | 0.5 | 0.3  | 0.4     | 0.3             | 0.2  | 0.3     | 2.9              | 2.7  | 2.9     |
| (6) RPur                        | 3.0              | 8.7   | 6.1     | 0.1 | 0.4  | 0.3     | 0.0             | 0.3  | 0.3     | 1.1              | 4.6  | 3.6     |
| (7) RNeg                        | 0.6              | 2.7   | 1.0     | 0.2 | 0.8  | 0.6     | 0.1             | 0.6  | 0.4     | 1.7              | 6.1  | 3.6     |
| (8) RMad                        | 7.2              | 13.9  | 18.5    | 0.6 | 0.5  | 0.8     | 2.7             | 3.0  | 4.3     | 1.7              | 5.2  | 6.8     |
| (9) OBi                         | 74.6             | 151.1 | 131.5   | 8.2 | 9.3  | 9.0     | 9.7             | 8.6  | 15.2    | 23.8             | 46.1 | 38.1    |

Edmond (1981), sampling only the event water of local precipitation along a longitudinal transect of the river on two separate cruises (May–June 1976 and May 1977).

Recent chemical analysis of precipitation from Mortatti (1995) was based on a sampling network of eight stations distributed all over the basin, during the year 1989. A composite sample was collected and analysed every 15 days. For each major element, there is a decreasing concentration gradient going from the Atlantic ocean to the continent comparable to those previously calculated by Stallard and Edmond (1981). The chemical composition of the precipitation over the different major tributary basins was estimated using these gradients on the basis of their average distance from the ocean. Results are shown in Table 3, expressed in  $\mu\text{M l}^{-1}$  concentration, and the mean values are weighted by the total annual rainfall (WPM).

To check on the validity of basin-wide calculations, the mean values obtained for each tributary were compared with average concentration obtained for the whole basin at Óbidos. When summing the different tributary rainfall concentration, weighted by their respective amount of precipitation, one recovers 93%

Table 3

Average chemical composition (in  $\mu\text{M l}^{-1}$ ) of the atmospheric precipitation calculated for the year 1989 in each Amazon sub-basin, using the measurements made by Mortatti (1995) on a sampling network of eight stations and on the concentration gradients from the coast to the interior of the continent (see text for the method of calculation)

| Basin    | SO <sub>4</sub> | Cl   | Ca   | Mg   | Na   | K    | Rainfall |
|----------|-----------------|------|------|------|------|------|----------|
| (1) VGr  | 7.83            | 3.05 | 4.55 | 0.03 | 4.63 | 3.57 | 2238     |
| (2) RIça | 8.16            | 3.90 | 4.70 | 0.38 | 5.57 | 3.78 | 3000     |
| (3) RJut | 8.58            | 5.32 | 4.88 | 0.83 | 7.00 | 4.04 | 2500     |
| (4) RJur | 8.33            | 4.42 | 4.77 | 0.56 | 6.10 | 3.88 | 2400     |
| (5) RJap | 8.25            | 4.15 | 4.73 | 0.47 | 5.83 | 3.83 | 3000     |
| (6) RPur | 8.67            | 5.66 | 4.91 | 0.92 | 7.33 | 4.09 | 2280     |
| (7) RNeg | 8.92            | 6.82 | 5.02 | 1.18 | 8.41 | 4.24 | 2533     |
| (8) RMad | 8.79            | 6.21 | 4.97 | 1.05 | 7.85 | 4.17 | 1859     |
| WPM      | 8.42            | 4.88 | 4.81 | 0.66 | 6.53 | 3.94 | 2261     |
| (9) OBi  | 8.58            | 5.32 | 4.88 | 0.83 | 7.00 | 4.17 | 2200     |
| d%       | 1.9             | 8.6  | 1.4  | 22.8 | 6.9  | 5.7  | 2.7      |

Rainfall is the corresponding amount of annual precipitation (in mm/year). WPM is the mean chemical composition calculated for the whole Amazon basin by weighting the values obtained for each sub-basin by the annual rainfall height. WPM is compared with the average concentration obtained directly for the whole Amazon basin at Óbidos (station 9). d% is the difference in % between WPM and Óbidos.



of the total rainfall inputs over the whole basin at Óbidos.

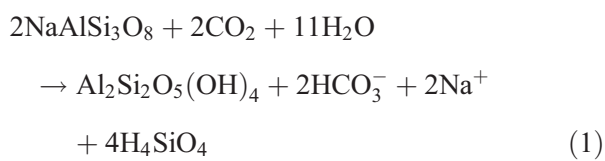
The contribution of the atmospheric inputs to the dissolved load transported by the Amazon river to the ocean was estimated for each chemical species to 56.9% for  $\text{SO}_4^{2-}$ , 21.9% for  $\text{Cl}^-$ , 6.0% for  $\text{Ca}^{2+}$ , 3.7% for  $\text{Mg}^{2+}$ , 13.8% for  $\text{Na}^+$  and 32.3% for K. The atmospheric inputs of  $\text{Na}^+$ ,  $\text{Ca}^{2+}$ ,  $\text{Mg}^{2+}$ ,  $\text{SO}_4^{2-}$  and  $\text{Cl}^-$  are related to the cyclic salts and those of  $\text{K}^+$  to terrestrial emissions derived inside the basin.

After corrections for atmospheric input (including  $\text{CO}_2$ ), the mean riverine transport of dissolved material by the Amazon was calculated as  $148.9 \times 10^6$  tons/year, i.e. 32.2 tons/ $\text{km}^2$ /year. This weathering flux represents 59% of the total dissolved river load carried out to the ocean.

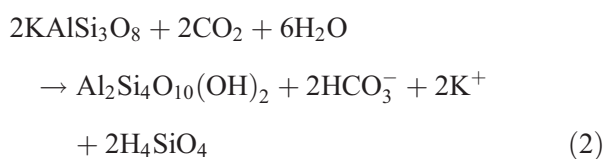
## 5. $\text{CO}_2$ consumption by rock weathering

The natural weathering pathway derived from the reaction of the carbonic acid on minerals to produce dissolved inorganic carbon (mainly  $\text{HCO}_3^-$ ) is largely reported in the literature (Garrels and Mackenzie, 1971; Holland, 1978; Gac, 1980; Berner et al., 1983; Tardy, 1986; Meybeck, 1987; Probst, 1992; Probst et al., 1994, 1997; Amiotte Suchet and Probst, 1995; Mortatti et al., 1997; Ludwig et al., 1999). The classical weathering reactions of silicate mineral hydrolysis (Eqs. (1)–(4)) and carbonate mineral dissolution (Eq. (5)) are related to the alkalinity production during this process:

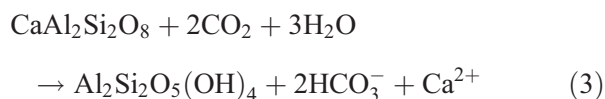
– albite into kaolinite:



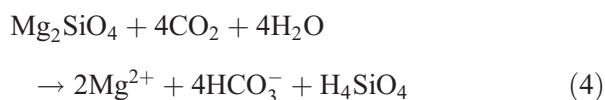
– K-feldspar into montmorillonite:



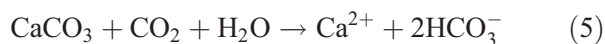
– Ca-plagioclase into kaolinite:



– Olivine weathering:



– calcite dissolution:



The flux of  $\text{CO}_2$  consumed by weathering processes is mainly produced by soil organic matter oxidation which releases carbonic acid:



All  $\text{HCO}_3^-$  produced by silicate weathering (Eqs. (1)–(4)) is from the atmospheric/soil origin via organic matter oxidation (Eq. (6)), whereas for carbonate dissolution (Eq. (5)), only half of  $\text{HCO}_3^-$  released are from the atmospheric/soil  $\text{CO}_2$ .

For the Amazon basin at Óbidos, the contribution of atmospheric/soil  $\text{CO}_2$  to the total  $\text{HCO}_3^-$  river fluxes can be estimated in four ways:

- (1) based on partial budgets of input–output  $\text{HCO}_3^-$  fluxes from the different tributaries to the main channel of Solimões/Amazon river;
- (2) based on a global budget of the fluxes of dissolved chemical species at Óbidos (Stallard, 1980; Probst et al., 1994; Mortatti, 1995);
- (3) based on geochemical modeling (MEGA), using weathering reactions of the principal minerals (Amiotte Suchet, 1995; Amiotte Suchet and Probst, 1996);
- (4) based on mathematical inversion of chemical data (Gaillardet et al., 1997).

The calculation procedure used for the Amazon basin follows the same assumptions made by Stallard

(1980) and Probst et al. (1994). After cyclic salt correction, one makes the following hypotheses (all element fluxes are expressed in mol/year):

- all chloride ( $F_{Cl}$ ) is from the halite dissolution;
- after subtraction of the NaCl component, all sodium is derived from silicate rock weathering ( $F_{Na\ sil}$ );
- all potassium ( $F_K$ ) is derived from silicate weathering ( $F_K\ sil$ );
- calcium and magnesium are derived from carbonate ( $F_{Ca\ carb}$  and  $F_{Mg\ carb}$ ) and evaporite dissolution, and from silicate hydrolysis ( $F_{Ca\ sil}$  and  $F_{Mg\ sil}$ ).

Following these assumptions, the total atmospheric/soil  $CO_2$  ( $F_{CO_2}$ ) consumed by the rock weathering (carbonate plus silicate) was calculated by the following equation:

$$F_{CO_2} = F_{Na\ sil} + F_K\ sil + 2F_{Mg\ sil} + F_{Mg\ carb} + 2F_{Ca\ sil} + F_{Ca\ carb} \quad (7)$$

In this equation, the factors 1 (for Na and K released by silicate weathering and for Ca and Mg released by carbonate dissolution) or 2 (Ca and Mg released by silicate weathering) affected to each flux  $F$  are derived from the stoichiometric coefficients (cations released versus alkalinity produced from atmospheric  $CO_2$ ) of weathering reactions (Eqs. (1)–(4) for silicate and Eq. (5) for carbonate).

The main difficulty in such an approach is to distinguish between Ca and Mg contribution of silicate weathering and carbonate dissolution to the total Ca and Mg riverine fluxes. The contribution of silicate weathering to the fluxes of Ca + Mg can be calculated by using the ionic ratio  $(Na + K)/(Ca + Mg)$  in stream water draining only silicate rocks (Probst et al., 1994; Amiotte Suchet, 1995; Amiotte Suchet and Probst, 1996) or by using the average ratio Ca/Na and Mg/Na of fresh water draining shield basements (Négrel et al., 1993; Mortatti et al., 1997; Boeglin et al., 1997). In this study, we used the ionic ratios  $Ca/Na = 0.575$  and  $Mg/Na = 0.304$  as calculated by Boeglin et al. (1997) on the basis of literature data (Feth et al., 1964; Tardy, 1969, 1971; Drever, 1997).

The results obtained concerning the atmospheric/soil  $CO_2$  consumed by carbonate dissolution ( $F_{CO_2\ carb}$ ), by silicate weathering ( $F_{CO_2\ silicate}$ ) and

by the total rock weathering (silicate plus carbonate:  $F_{CO_2\ total}$ ) are reported in Table 4 for the low and high river water periods. As seen in Fig. 6, the riverine alkalinity concentrations that can be calculated using the geochemical modeling are close to the concentrations measured in the different rivers. Also shown in Table 4 are the contribution (%) of atmospheric/soil  $CO_2$  consumption (carbonate plus silicate) to the total alkalinity river fluxes in the Amazon basin and the mean specific fluxes of  $CO_2$  uptake ( $F_{CO_2\ silicate}$ ) and dissolved elements (CE silicate) released by chemical erosion of silicates into the river water, with their respective values for low and high river water periods. CE silicate (in tons/ $km^2$ /year) is calculated as follows:

$$CE\ silicate = TDS\ silicate / S \quad (8)$$

where TDS (in tons/year) is the sum of cation, silica and alkalinity fluxes (tons/year) calculated using the geochemical modeling (particularly for Ca, Mg and alkalinity produced by silicate weathering) and  $S$  is the drainage basin area ( $km^2$ ).

Considering only the silicate rocks, the specific fluxes (in mol/ $km^2$ /year or tons/ $km^2$ /year) of dissolved elements (CE silicate) and of  $CO_2$  consumption ( $F_{CO_2\ silicate}$ ) can be calculated by simplification by dividing the flux by the total basin area rather than by the silicate rock area because the silicate rocks occupy 94–100% of the total basin area according to the river basin (96.1% for the Amazon basin at Óbidos). This means that we underestimate some % of the  $CO_2$  flux and the chemical erosion of silicates when dividing the fluxes by the total drainage basin area, except for the Negro river which is associated with silicate weathering only, because its basin drains mainly shield terrains.

These results show that at Óbidos, the average contribution of the atmospheric/soil  $CO_2$  to the total alkalinity river flux is around 68%, which corresponds to a total atmospheric/soil  $CO_2$  ( $F_{CO_2\ total}$ ) consumed by rock weathering of  $331 \times 10^3$  mol/ $km^2$ /year.

This specific  $CO_2$  flux is higher than that calculated by Amiotte Suchet and Probst (1995), who used a modeling approach GEM- $CO_2$  ( $271 \times 10^3$  mol/ $km^2$ /year) based on empirical relationships between weathering  $CO_2$  flux and river discharge determined for each rock type (Amiotte Suchet and Probst, 1993a,b, 1995). The difference between the

Table 4

Total alkalinity river fluxes ( $F_{\text{HCO}_3}$ , total) and atmospheric/soil  $\text{CO}_2$  fluxes ( $F_{\text{CO}_2}$ , atm total) consumed by the rock weathering (silicate plus carbonate) with their respective contribution (%) to  $F_{\text{HCO}_3}$ , total

| River basin | $F_{\text{HCO}_3}$ , total ( $10^9$ mol/year) * |      |         | $F_{\text{CO}_2}$ , atm total               |      |         | $F_{\text{CO}_2}$ , silicate ( $10^3$ mol/km <sup>2</sup> /year) |      |         | CE silicate (tons/km <sup>2</sup> /year) |      |         |      |      |
|-------------|---|------|---------|---|------|---------|--|------|---------|--|------|---------|------|------|
|             | Low   | High | Average | Low   | High | Average | Low  | High | Average | Low                                      | High | Average |      |      |
|             | % $F_{\text{HCO}_3}$ , total                    |      |         | (10 <sup>3</sup> mol/km <sup>2</sup> /year) |      |         |  |      |         |  |      |         |      |      |
| (1) VGr     | 703   | 1451 | 1519    | 59.3  | 63.5 | 62.9    | 368  | 812  | 842     | 115                                      | 345  | 17.6    | 41.7 | 40.9 |
| (2) RIça    | 19  | 27   | 21      | 91.7  | 66.3 | 65.2    | 115  | 122  | 94      | 104                                      | 47   | 16.8    | 16.3 | 14.0 |
| (3) RJur    | 2   | 10   | 13      | 60.2  | 54.2 | 53.1    | 12   | 68   | 93      | 4  | 7    | 6.1     | 12.4 | 12.6 |
| (4) RJur    | 34  | 100  | 83      | 57.9  | 69.1 | 64.4    | 92   | 322  | 244     | 28                                       | 180  | 3.8     | 22.3 | 15.1 |
| (5) RJap    | 45  | 45   | 70      | 84.3  | 90.1 | 79.4    | 131  | 142  | 194     | 107                                      | 128  | 18.8    | 21.6 | 21.4 |
| (6) RPur    | 49  | 151  | 97      | 85.4  | 78.3 | 75.6    | 113  | 317  | 196     | 94                                       | 228  | 10.4    | 31.3 | 20.8 |
| (7) RNeg    | 37  | 147  | 48      | 100   | 100  | 100     | 49   | 195  | 64      | 49                                       | 195  | 4.4     | 24.1 | 7.4  |
| (8) RMav    | 119   | 244  | 334     | 93.6  | 78.6 | 74.7    | 80   | 139  | 180     | 74                                       | 101  | 7.4     | 12.2 | 14.9 |
| (9) OBi     | 1455  | 2693 | 2254    | 78.4  | 72.8 | 67.8    | 247  | 425  | 331     | 179                                      | 267  | 19.6    | 32.0 | 22.6 |

$F_{\text{CO}_2}$ , carbonate and  $F_{\text{CO}_2}$ , silicate are atmospheric/soil  $\text{CO}_2$  fluxes consumed respectively by carbonate dissolution silicate and by weathering only. CE is the chemical denudation rates of silicates (CE silicate) for the Amazon river and its main tributaries. Mean values are given for the average year and for low and high river water periods.

\*  $F_{\text{HCO}_3}$ , total is calculated from the modeling.

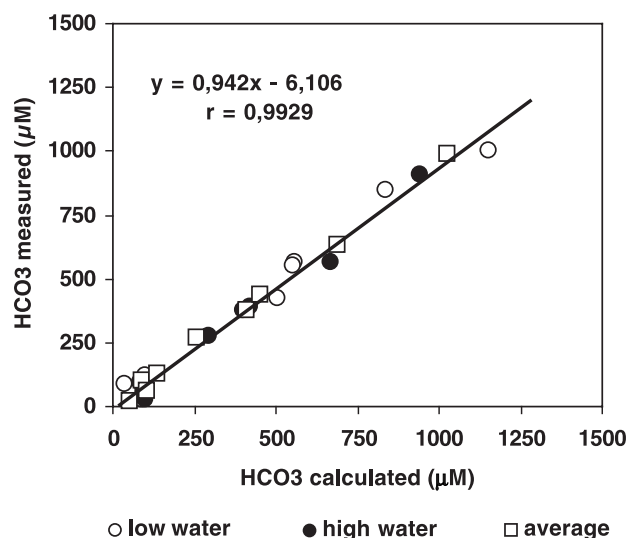


Fig. 6. Relationship between the bicarbonate concentrations (in  $\mu\text{M}$   $\text{l}^{-1}$ ) calculated for the Amazon river and its main tributaries using the geochemical modeling and the bicarbonate concentrations measured in the river waters during low, high and average water stages.

GEM- $\text{CO}_2$  simulation and our results can be explained by some simplifications of the geological map that Amiotte Suchet and Probst (1995) used. However, the contribution of the atmospheric  $\text{CO}_2$  to the alkalinity river flux calculated by GEM- $\text{CO}_2$  (68%) remains the same.

During the low water stage, the total  $F_{\text{CO}_2}$  consumed by the rock weathering, at Óbidos station, was  $247 \times 10^3$  mol/km<sup>2</sup>/year, while during the high water period, this value was around  $425 \times 10^3$  mol/km<sup>2</sup>/year. The same pattern can be observed in the upper stream, at Vargem Grande station, with 368 and  $812 \times 10^3$  mol/km<sup>2</sup>/year, respectively, for low and high water periods. Significant contributions of Madeira, Juruá and Purus rivers can be observed, while the Negro river contribution (shield) is of little importance. The value obtained for the Madeira river basin, during high water period ( $139 \times 10^3$  mol/km<sup>2</sup>/year), is very close to the value ( $141 \times 10^3$  mol/km<sup>2</sup>/year) given by Gaillardet et al. (1997) for the high water stage of May 1989. These  $\text{CO}_2$  flux variations that can be observed between the upper part of the Amazon basin and the lower part have already been simulated by Amiotte Suchet and Probst (1995) using GEM- $\text{CO}_2$  on a grid resolution of  $50 \times 50$  km latitude/longitude over the whole Amazon basin (Fig. 7).

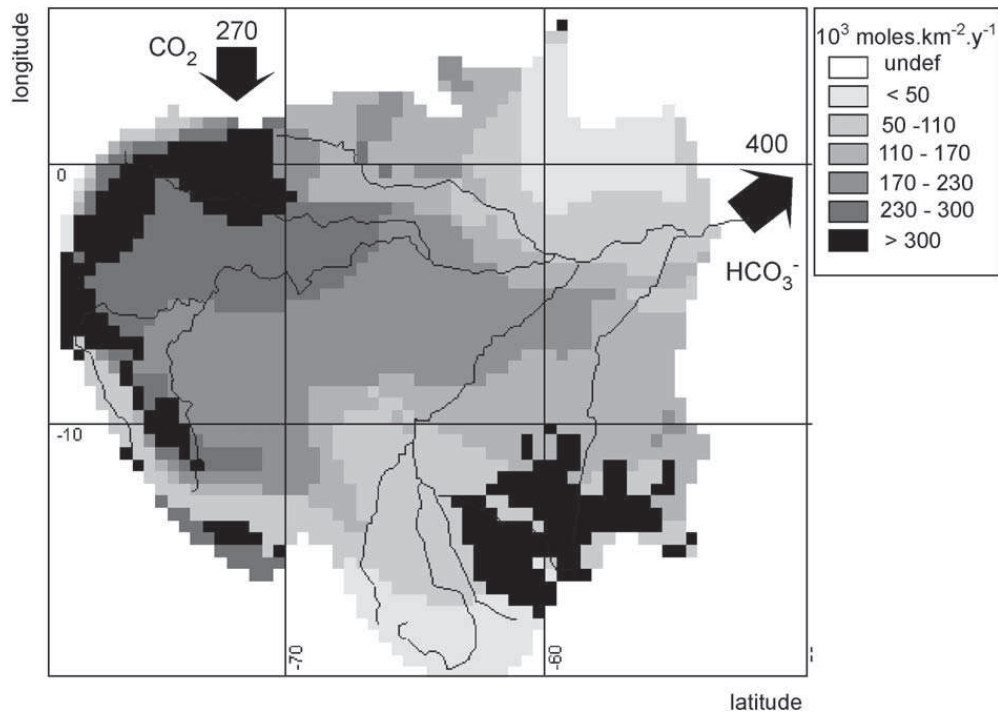


Fig. 7. Spatial distribution of atmospheric CO<sub>2</sub> consumed by chemical erosion in the Amazon basin (extracted from Amiotte Suchet and Probst, 1995).

Compared to the world continental averages ( $161 \times 10^3$  mol/km<sup>2</sup>/year for the total land area,  $800 \times 10^3$  mol/km<sup>2</sup>/year for carbonates and  $34 \times 10^3$  mol/km<sup>2</sup>/year for silicate rocks) that can be calculated from Meybeck's (1987) data, the Amazon CO<sub>2</sub> fluxes appear higher mainly because of the runoff intensity (mm/a) which is on average three times more important for the Amazon basin than for the whole continental areas. The results verified for the Amazon basin are very close to the values obtained previously by Stallard (1980), Amiotte Suchet and Probst (1993b) and Probst et al. (1994).

The riverine specific transport of dissolved elements released by silicate weathering (CE silicate) for the whole Amazon basin was estimated at Óbidos (station 9) to 22.6 tons/km<sup>2</sup>/year (Table 4), while in the upper part of the basin, at Vargem Grande (station 1), the silicate specific transport is higher and reaches 40.9 tons/km<sup>2</sup>/year. During the low water period, the silicate specific transports were lower than that observed during the high river water stage, 17.6 and 41.7 tons/km<sup>2</sup>/year, respectively, for Vargem Grande, and 19.6 and 32 tons/km<sup>2</sup>/year, respectively, for Óbidos. At Santarém, near Óbidos, the result obtained

by Gaillardet et al. (1997) for this specific transport was only about 15 tons/km<sup>2</sup>/year.

Fig. 8A shows that there is a good relationship between the mean specific flux of atmospheric/soil CO<sub>2</sub> consumed by silicate weathering ( $F_{\text{CO}_2}$  silicate) and the amount of major elements released by silicate weathering (CE silicate). It can be observed that the Amazon at Óbidos results in a mixing between the shield and Amazon trough tributaries, which present low silicate riverine transport and low CO<sub>2</sub> fluxes, and the Andean tributaries which exhibit higher fluxes. The same behavior cannot be observed if one distinguishes low and high river water stages (Fig. 8B), but it appears a significant linear correlation between  $F_{\text{CO}_2}$  silicate (10<sup>3</sup> mol/km<sup>2</sup>/year) and CE silicate (tons/km<sup>2</sup>/year):

$$F_{\text{CO}_2} \text{ sil} = 8.398 \text{ CE silicate} - 22.852$$

with  $r = 0.9355$  and  $p = 0.01\%$  (9)

The specific  $F_{\text{CO}_2}$  silicate flux shows also a good logarithmic correlation with the discharge values ( $Q$

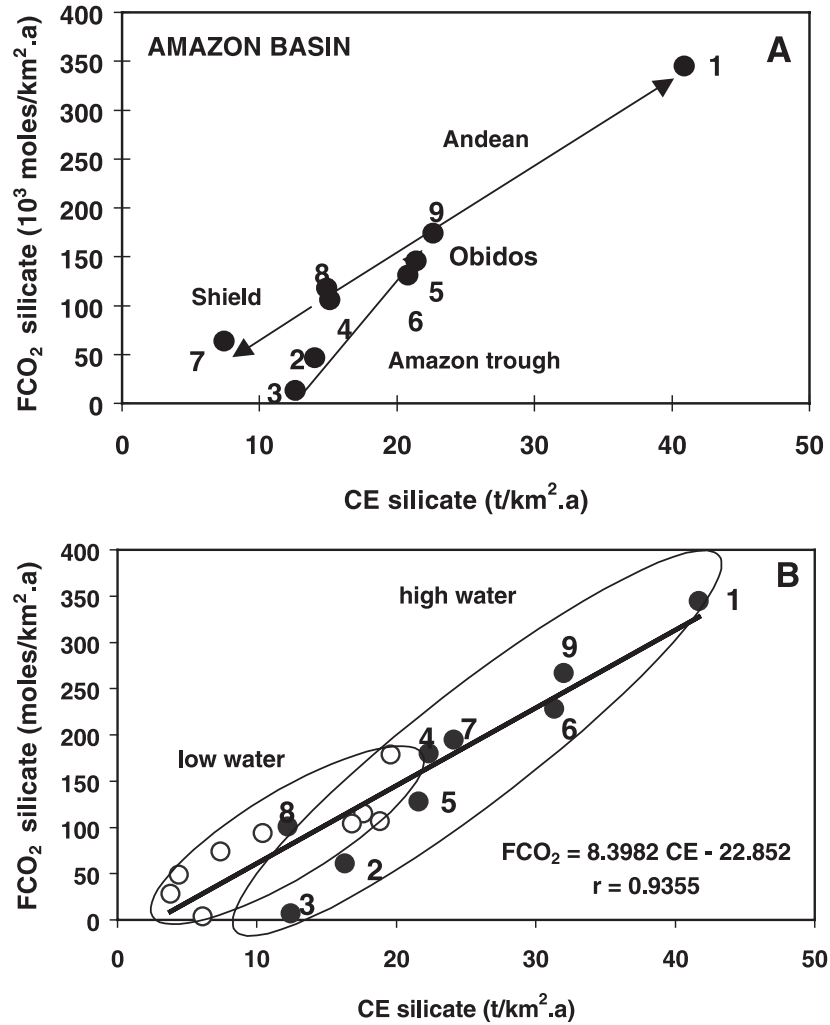


Fig. 8. Relationships between the mean flux of atmospheric/soil CO<sub>2</sub> consumed during the silicate weathering ( $F_{CO_2}$ ) and the mean specific silicate erosion (CE) for the Amazon basin. (A) Annual average values. (B) Values for the low and high river water periods. 1—Solimões river at Vargem Grande; 2—Iça; 3—Jutai; 4—Juruá; 5—Japurá; 6—Purus; 7—Negro; 8—Madeira; 9—Amazon river at Óbidos.

in m<sup>3</sup>/s) of the Amazon and main tributaries, considering low and high river water periods together (Fig. 9):

$$F_{CO_2} \text{ sil} = 48.46 \ln Q - 328.43$$

with  $r = 0.7465$  and  $p = 0.1\%$  (10)

## 6. Weathering rates of silicate rocks

In order to determine the main weathering types occurring in the Amazon basin from the geochemistry

of river waters, we used a modified version (Boeglin et al., 1997; Boeglin and Probst, 1998) of the weathering index  $R_E$  proposed initially by Tardy (1968, 1971). This is based on the molecular ratio between dissolved silica and cations resulting from silicate rock weathering, including Mg to take into account of Mg-silicate minerals such as amphiboles:

$$RE = \frac{3K + 3Na + 2Ca + 1.25Mg - SiO_2}{0.5K + 0.5Na + Ca + 0.75Mg} \quad (11)$$

The different coefficients used in the above formula depend on the major primary minerals of the bedrock and corresponds here to an average

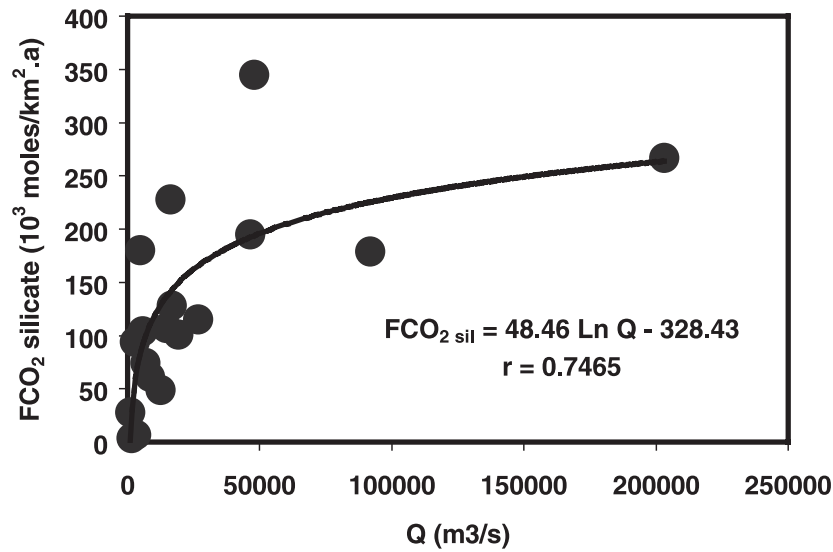


Fig. 9. Logarithmic relationship between the specific flux of atmospheric/soil CO<sub>2</sub> consumed during silicate weathering ( $F_{CO_2}$  silicate, in 10<sup>3</sup> mol/km<sup>2</sup>/year) and the river water discharge ( $Q$ , in m<sup>3</sup>/s) during low and high river water periods for the Amazon and its main tributaries.

granitic composition with feldspars and micas (see Tardy, 1971).  $R_E$  is also equivalent to the molar ratio SiO<sub>2</sub>/Al<sub>2</sub>O<sub>3</sub> of silica and aluminium oxides remaining in the weathering profile (Pedro, 1966). When  $R_E$  value decreases, more silica is evacuated and the chemical weathering stage of the minerals increases:  $R_E=4, 2$  and  $0$  correspond, respectively, to smectite, kaolinite and gibbsite genesis. The mean  $R_E$  value obtained for the Amazon basin was 2.1, which represents the monosiallitization weathering process corresponding to kaolinite formation in the soil profile. In the upper Solimões basin, near Vargem Grande, the mean  $R_E$  is slightly higher (2.4) than at Óbidos, indicating a tendency to bisiallitization process (formation of smectites), whereas for the Negro river basin, the monosiallitization weathering processes appear to be dominant ( $R_E=1.0$ ), indicating the kaolinite neoformation in the alteration profiles and gibbsite at the top of the soil profile. These results are in accordance with the mineralogical investigation of the riverine sediments deposited in the Amazon “varzea” as reported by Irion (1983), Franzinelli and Potter (1993) and Martinelli et al. (1993).

The mean annual dissolved SiO<sub>2</sub> carried out by the Amazon river to the ocean is calculated to be  $38.1 \times 10^6$  tons, corresponding to a specific riverine transport of 8.25 tons/km<sup>2</sup>/year.

The chemical weathering rate of silicate rocks ( $WR_{ch}$ ) can be calculated from the flux of dissolved silica in the river waters ( $F_{SiO_2}$ ), knowing the chemical composition of the parent rock ( $S_0$ ) and of the saprolite ( $S_S$ , alteration facies found at the bottom of lateritic profiles, mainly composed of neoformed kaolinite and residual quartz), and considering isovolumetric rock weathering, as described by Boeglin and Probst (1998):

$$WR_{ch} = F_{SiO_2} / (S_0 - S_S) \quad (12)$$

For the Amazon basin, the silica content in the parent rock and in the mean soil profile is 56.3 and 50.5%, respectively, given by Stallard (1980). With a density of 2.65 tons/m<sup>3</sup>, the amount of silica in the unweathered mean parent rock ( $S_0$ ) is 1490 kg/m<sup>3</sup>, while for the mean soil profile, with a density of 1.8 tons/m<sup>3</sup>, the amount of silica ( $S_S$ ) is about 909 kg/m<sup>3</sup>. Following the above method, one can calculate the mean chemical weathering rate of silicate rocks for the Amazon basin to 14.8 m/My on average, taking into account the occurrence of this rock type in the basin (96%, as estimated by Amiotte Suchet, 1995). The results reported in Table 5 show that this weathering rate varies in time and in space. For low and high river water stages, the values calculated for Óbidos station range between 9.4 and 18 m/My, respectively. For the

Table 5

Erosion balance of the Amazon basin and major tributary sub-basins, estimated during the period 1982–1984, using the particulate (TSS) and dissolved (TDS) loads transported by river water (in  $10^6$  tons/year)

| River basin | TSS                 | TDS                 | ME                           | CE                           | WR <sub>ph</sub> |       |         | WR <sub>ch</sub> |      |         |
|-------------|---------------------|---------------------|------------------------------|------------------------------|------------------|-------|---------|------------------|------|---------|
|             | ( $10^6$ tons/year) | ( $10^6$ tons/year) | (tons/km <sup>2</sup> /year) | (tons/km <sup>2</sup> /year) | (m/My)           |       |         | (m/My)           |      |         |
| Water level | Average             | Average             | Average                      | Average                      | Low              | High  | Average | Low              | High | Average |
| (1) VGr     | 579.4               | 103.2               | 510.7                        | 91.0                         | 102.0            | 215.0 | 255.0   | 15.0             | 24.7 | 23.7    |
| (2) RIça    | 19.8                | 2.8                 | 133.8                        | 25.7                         | 74.0             | 64.0  | 67.0    | 13.9             | 19.8 | 17.7    |
| (3) RJut    | 2.0                 | 1.6                 | 27.0                         | 21.6                         | 7.0              | 1.0   | 14.0    | 9.3              | 18.6 | 19.8    |
| (4) RJur    | 21.1                | 5.0                 | 97.2                         | 23.0                         | 4.0              | 45.0  | 49.0    | 2.4              | 13.4 | 10.8    |
| (5) RJap    | 25.2                | 5.9                 | 87.2                         | 20.4                         | 59.0             | 39.0  | 44.0    | 17.2             | 16.0 | 17.3    |
| (6) RPur    | 28.6                | 7.5                 | 76.9                         | 20.2                         | 6.0              | 12.0  | 38.0    | 5.2              | 21.3 | 17.0    |
| (7) RNeg    | 6.2                 | 6.4                 | 8.2                          | 8.5                          | 1.0              | 8.0   | 4.0     | 4.0              | 14.0 | 8.3     |
| (8) RMad    | 311.8               | 22.8                | 225.9                        | 16.5                         | 7.0              | 14.0  | 113.0   | 2.3              | 7.1  | 8.8     |
| (9) Obi     | 1140.0              | 148.9               | 246.9                        | 32.2                         | 29.0             | 135.0 | 123.0   | 9.4              | 18.0 | 14.8    |

ME and CE correspond respectively to the mechanical and chemical erosion calculated for the whole basins. WR<sub>ph</sub> and WR<sub>ch</sub> are respectively the physical and chemical weathering rates calculated only for the silicate rock areas.

different stations, the values vary from 8 m/My in the Amazon shield to 24 m/My in the Andes. These rates are comparable to those calculated by [Nkounkou and Probst \(1987\)](#) and [Probst \(1992\)](#) for the Congo basin (8.5 m/My for crystalline rocks and 12.6 m/My for sandstone), by [Freyssinet and Farah \(2000\)](#) for the Yaou basin in French Guyana (8 m/My), and by [Brauscher et al. \(2000\)](#) for the Cameroon and Gabon using <sup>10</sup>Be (12 m/My). However, they are higher than the rates calculated by [Boeglin and Probst \(1998\)](#) in an African tropical environment for the Niger river basin (4.7–6.1 m/My).

## 7. Chemical erosion versus physical erosion

[Fig. 10](#) illustrates the relationship between the mean chemical weathering rates (WR<sub>ch</sub>) as calculated previously and the mean mechanical erosion (WR<sub>ph</sub>). WR<sub>ph</sub> is estimated using the CAMREX data on river suspended sediment concentrations by dividing the total riverine flux of suspended sediments by the drainage basin area and by the average soil density ( $d=2$ ):

$$\text{WR}_{\text{ph}} \text{ (m/My)} = \frac{\text{TSS (tons/year)}}{(S(\text{km}^2) \times d \text{ (tons/m}^3))} \quad (13)$$

The lithologic basement associated with the mechanical and chemical erosions can be observed. For

the Andean part of the Amazon basin (Solimões and Madeira), and consequently for Óbidos, and to a lesser extent for the Amazon trough (Iça, Juruá, Japurá, and Purus), WR<sub>ph</sub> is largely superior to WR<sub>ch</sub> showing that the soil equilibrium is broken. On the contrary, for the shield tributaries (Jutaí and Negro), the WR<sub>ch</sub> and WR<sub>ph</sub> are close to the equilibrium but indicating that WR<sub>ch</sub> is slightly superior to WR<sub>ph</sub>.

The erosion balance (mechanical versus chemical) calculated for the Amazon basin at Óbidos, and for the major tributary sub-basins, can be summarized in [Table 5](#). This table presents the main results obtained for silicate rocks in terms of particulate and dissolved loads transported by river water, specific riverine transports and mechanical and chemical weathering rates.

The mean results obtained for the whole Amazon basin illustrate the importance of specific solid transports (246.9 tons/km<sup>2</sup>/year), being eight times higher than the specific dissolved transports (32.2 tons/km<sup>2</sup>/year). On average, the particulate riverine transports represent about 88% of the total riverine transport in the basin, showing the great influence of the Andean complex in upstream part of the drainage basin. This becomes more evident if one compares the mean physical denudation rate of silicate rocks at the top of the soil profile (WR<sub>ph</sub>) with the mean chemical weathering rate at the bottom of the soil profile (WR<sub>ch</sub>) ([Table 5](#)).

For the whole Amazon basin, the mean soil denudation rate was calculated as being 123 m/My (ranged

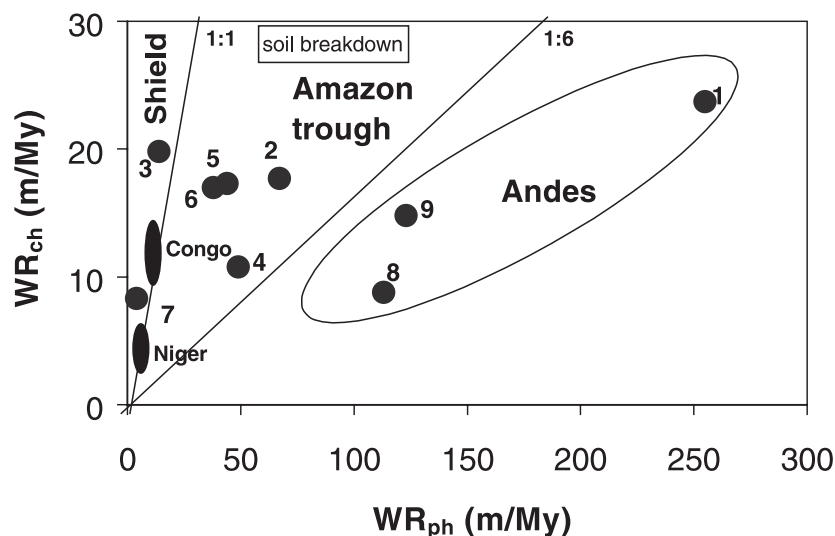


Fig. 10. Relationship between the mean physical denudation ( $WR_{ph}$ ) and mean chemical weathering rates ( $WR_{ch}$ ) for the Amazon basin and its main subbasins. Comparison with the Congo (data from Nkounkou and Probst, 1987) and Niger (data from Boeglin and Probst, 1998) river basins. 1—Solimões river at Vargem Grande; 2—Iça; 3—Jutaí; 4—Juruá; 5—Japurá; 6—Purus; 7—Negro; 8—Madeira; 9—Amazon river at Óbidos.

between 29 and 135 m/My), higher than the chemical weathering rate, 14.8 m/My (ranged between 9.4 and 18 m/My), corresponding to soil breakdown. This means that the soils of the Amazon basin are not in equilibrium and their thickness tend to be reduced on average in present-day conditions as shown by Gaillardet et al. (1997). On the contrary, for the Negro river, draining mainly the shield complex, this behavior is opposite, showing a disequilibrium between mechanical and chemical erosion rates in favour of the chemical weathering, corresponding to a soil deepening.

Nevertheless, some uncertainties on these  $WR_{ch}/WR_{ph}$  ratio calculations remain. Indeed,  $WR_{ph}$  is calculated using the river sediment loads and is probably underestimated, particularly for the station located at the exutory of the Amazon basin, because part of the sediments eroded in the Andes can be stored in the Amazon floodplain along the river valley. According to Dunne et al. (1998), the net balance of the two main processes (bank erosion and floodplain sedimentation) of sediment exchange between the channel and the floodplain is estimated to be  $500 \times 10^6$  tons/year of sediments deposited in the Amazon floodplain until Óbidos station. This means that 30% of the sediments which are eroded in the Andes and transported by the Amazon river and its

tributaries could be deposited in the Amazon floodplain. Consequently, our  $WR_{ph}$  calculations could be underestimated of 30% maximum, particularly for the Amazon basin at Óbidos, but less for the upper parts of the basin. Concerning  $WR_{ch}$ , the calculation is based on the riverine silica flux and on the silica mass balance between the soil profile and the bedrock. Nevertheless, the validity of this method of calculation is limited by several conditions (isovolumetric weathering, all primary minerals are transformed into kaolinite, riverine silica is conservative, all riverine silica is produced by rock weathering) as already mentioned by Boeglin and Probst (1998). Moreover, this calculation is sensitive to the chemical and mineralogical composition of the bedrock that could not be considered in detail at the scale of the Amazon basin. Indeed the percentage of silica is different from one silicate rock to another and the difference between the silica content in the bedrock ( $S_0$  in Eq. (12)) and in the saprolite ( $S_S$ ) could vary according to the parent rock. If the parent rock is a recycled sediment like the sediments deposited in the Amazon trough near the Andes,  $S_0 - S_S$  might be lower and, consequently,  $WR_{ch}$  might be also underestimated. Moreover, as shown by Boeglin and Probst (1998), the percentage of quartz remaining in the soil profile plays an important role in the  $WR_{ch}$  calculation. Considering



a 15% dissolution ratio of the bedrock quartz, they show that  $WR_{ch}$  could be 1.7 time higher than if a complete quartz dissolution is considered (i.e. no quartz remaining in the saprolite). Finally, the underestimation of  $WR_{ph}$  due to sediment deposition in the floodplain could be partly compensated by the underestimation of  $WR_{ch}$  due to different mineralogical compositions of the parent rocks and to residual quartz in the soil profiles.

Nevertheless, taking these uncertainties into account, the influence of the Amazon plains on the mean erosion balance shows an important reduction of the mechanical erosion around 48%, which confirms the significant chemical erosion occurring in this area. This predominance of chemical weathering confirms the previous study of [Stallard and Edmond \(1983\)](#), who already showed that the lithologic basement associated with the erosion mechanisms exert a major control on the river water chemistry in the drainage basin, in spite of the influences of the atmospheric inputs, particularly important for some elements.

## 8. Conclusion

The silicate rock weathering processes and the associated consumption of atmospheric/soil  $CO_2$  could be assessed in the Amazon basin using the river water geochemistry of the Amazon river and of its main tributaries. A geochemical modeling based on the stoichiometry of different mineral weathering reactions estimates the contribution of the atmospheric/soil  $CO_2$  at 68% of the total riverine alkalinity for the Amazon at Óbidos. This contribution varies from 53% for the Jutai to 100% for the Negro, as a function of the silicate outcrop abundance. The main results obtained in this study show that the weathering rates and the  $CO_2$  fluxes vary greatly in time and in space.

The seasonal variations show that the silicate weathering processes are highly controlled by the runoff fluctuations: high water periods correspond to high weathering rates and to high  $CO_2$  fluxes, as already shown by [Amiotte Suchet and Probst \(1993a,b, 1995\)](#) and [White and Blum \(1995\)](#) for small monolithologic watersheds. The ratio between high and low flows vary from 1 to 6 for both weathering rates and  $CO_2$  fluxes according to the lithology of the

drainage basin (highest values for sand and sandstone) and to the amplitude of the hydroclimatic seasonal variations. These results suggest also that the fluctuation amplitude could vary over the same range between humid and dry years. Consequently, some differences observed in the literature for previous studies on the Amazon basin may be due to these seasonal and interannual fluctuations.

The spatial variations exhibit the important role of the Andes in the global biogeodynamic of the Amazon basin, showing for the first time that the silicate weathering rate and the atmospheric/soil  $CO_2$  consumption are higher in the Andes than in the rest of the Amazon basin. Indeed, 80–90% of the total dissolved solids (of which the alkalinity represents 52%) transported by the Amazon river at Óbidos originate from the Andes. In the same way, the  $CO_2$  uptake by silicate rock weathering in the Andes represents 78% of the total flux of  $CO_2$  consumed by silicate rock weathering over the whole Amazon basin. This result confirms the hypothesis that the formation of mountains could play a major role in the  $CO_2$  content in the atmosphere and in the Earth climate evolution ([Raymo and Ruddimann, 1992](#); [Edmond, 1992](#)).

The chemical weathering rates of silicate rocks (rate of bedrock transformation into saprolite) calculated for the Amazon basin (8 m/My in the Shield to 24 m/My in the Andes, 15 m/My on average for the whole basin) is comparable to other estimations made for other humid tropical–equatorial river basins in Guyana and in Africa, but they are higher than weathering rates estimated for dry tropical environments like for the Niger river basin. A comparison between physical and chemical weathering rates of silicate rocks for the Amazon basin and for each tributary basin allows to determine on average if the soil thickness is increasing or decreasing even if it remains some uncertainties on the calculation of the weathering rates. The results show that in the Andes and in the Amazon trough, the soil thicknesses are decreasing whereas in the Shield the soil profiles are deepening like in the Congo and in the Niger river basins. Nevertheless, there is no clear relationship between chemical weathering rates and mechanical denudation rates contrary to what has been observed by [Gaillardet et al. \(1999b\)](#) for major world river basins.

## Acknowledgements

This study has been supported by a Conselho Nacional de Desenvolvimento Científico e Tecnológico (CNPq/Brazil) research grant and by a COFE-CUB international cooperation agreement (no. UC39/97) between CENA/USP in Brazil and CNRS in France. The authors would like to thank the reviewers, J. Gaillardet and R.F. Yuretich, and the editor, L. Walter, for their very helpful corrections and comments. This paper is also a contribution to the Working Group “Weathering as a Carbon Sink” of INQUA Carbon Commission and to the IGCP no. 459 on the “Carbon Cycle and Hydrology in the Paleo-Terrestrial Environments” (2001–2005). [LW]

## References

- Amiotte Suchet, P., 1995. Cycle du Carbone, Érosion Chimique des Continents et Transports vers les Océans. *Sci. Géol., Mem.* 97 (Strasbourg, 156 pp.).
- Amiotte Suchet, P., Probst, J.L., 1993a. Flux de CO<sub>2</sub> Consommé par Altération Chimique Continentale: Influences du Drainage et de la Lithologie. *C. R. Acad. Sci., Sér. II, Paris t.* 317, 615–622.
- Amiotte Suchet, P., Probst, J.L., 1993b. Modelling of atmospheric CO<sub>2</sub> consumption by chemical weathering of rocks: application to the Garonne, Congo and Amazon Basins. *Chem. Geol.* 107, 205–210.
- Amiotte Suchet, P., Probst, J.L., 1995. A global model for present-day atmospheric/soil CO<sub>2</sub> consumption by chemical erosion of continental rocks (GEM-CO<sub>2</sub>). *Tellus* 47B (1/2), 273–280.
- Amiotte Suchet, P., Probst, J.L., 1996. Origines du Carbone Inorganique Dissous dans les Eaux de la Garonne: Variations Saisonnières et interannuelles. *Sci. Géol., Bull., Strasbourg* 49 (1–4), 101–126.
- Amiotte Suchet, P., Probst, J.L., Ludwig, W., in press. World wide distribution of continental rock lithology: implications for the atmospheric/soil CO<sub>2</sub> uptake by continental weathering and alkalinity river transport to the oceans. *Glob. Biogeochem. Cycles*.
- Berner, R.A., 1994. GEOCARB II: a revised model of atmospheric CO<sub>2</sub> over Phanerozoic time. *Am. J. Sci.* 294, 56–91.
- Berner, R.A., Kothavala, Z., 2001. GEOCARB III: a revised model of atmospheric CO<sub>2</sub> over Phanerozoic time. *Am. J. Sci.* 301, 182–204.
- Berner, R.A., Lasaga, A.C., Garrels, R.M., 1983. The carbonate silicate geochemical cycle and its effect on atmospheric carbon dioxide over the past 100 millions years. *Am. J. Sci., New Haven* 283, 641–683.
- Boeglin, J.L., Probst, J.L., 1998. Physical and chemical weathering rates and CO<sub>2</sub> consumption in a lateritic environment: the upper Niger Basin. *Chem. Geol.* 148 (3–4), 137–156.
- Boeglin, J.L., Mortatti, J., Tardy, Y., 1997. Erosion Chimique et Mécanique sur le bassin amont du Niger (Guinée, Mali). Bilan Géochimique de l’altération en milieu tropical. *C. R. Acad. Sci., Paris* 325, 185–191.
- Brasil, 1987. Ministério das Minas e Energia; Departamento Nacional de Águas e Energia Elétrica; Divisão de Controle de Recursos Hídricos. Inventário das Estações Fluviométricas. Brasília, Dnaee, 1v.
- Braucher, R., Bourlès, D.L., Brown, E.T., Colin, F., Muller, J.P., Braun, J.J., Delaune, M., Edou Minko, A., Lescouet, C., Raisbeck, G.M., Yiou, F., 2000. Application of in situ-produced cosmogenic <sup>10</sup>Be and <sup>26</sup>Al to the study of lateritic soil development in tropical forest: theory and examples from Cameroun and Gabon. *Chem. Geol.* 170 (1–4), 95–111.
- Dessert, C., Dupré, B., François, L.M., Schott, J., Gaillardet, J., Chakrapani, G., Bajpai, S., 2001. Erosion of Decan Traps determined by river geochemistry: impact on the global climate and the <sup>87</sup>Sr/<sup>86</sup>Sr ratio of seawater. *Earth Planet. Sci. Lett.* 188, 459–474.
- Devol, H.A., Quay, P.D., Richey, J.E., Martinelli, L.A., 1987. The role of gas exchange in the inorganic carbon, oxygen, and <sup>222</sup>Rn budgets of the Amazon river. *Limnol. Oceanogr.*, Grafton 32 (1), 235–248.
- Drever, J.I., 1997. The Geochemistry of Natural Waters. Surface and Groundwater Environments, 3rd ed. Prentice-Hall, New Jersey, USA. 436 pp.
- Dunne, T., Mertes, L.A.K., Meade, R.H., Richey, J.E., Forsberg, B.R., 1998. Exchanges of sediment between the floodplain and channel of the Amazon river in Brazil. *Geol. Soc. Amer. Bull.* 110 (4), 450–467.
- Edmond, J.M., 1992. Himalayan tectonics, weathering processes, and the strontium isotope record in marine limestones. *Science* 258, 1594.
- Feth, J.H., Robertson, C.E., Polzer, W.L., 1964. Sources of mineral constituents in water from granitic rocks, Sierra Nevada, California and Nevada. *U. S. Geol. Surv. Water-Supply Pap.* 1535-I (70 pp.).
- François, L.M., Walker, J.C.G., 1992. Modeling of the Phanerozoic carbon cycle and climate: constraints from the <sup>87</sup>Sr/<sup>86</sup>Sr isotopic ratio of the seawater. *Am. J. Sci.* 292, 81–135.
- Franzinelli, E., Potter, P.E., 1993. Petrology, chemistry and texture of modern river sands, Amazon river system. *J. Geol., Chicago* 91, 23–39.
- Freyssinet, P., Farah, A.S., 2000. Geochemical mass balance and weathering rates of ultramafic schists in Amazonia. *Chem. Geol.* 170 (1–4), 133–151.
- Gac, J.Y., 1980. Géochimie du Bassin du Lac Tchad. Bilan de L’altération, de la Erosion et de la Sédimentation. *Trav. Doc. ORSTOM, Paris* (123), 1–251.
- Gaillardet, J., Dupré, B., Allègre, C.J., 1995. A global geochemical mass budget applied to the Congo basin rivers: erosion rates and continental crust composition. *Geochim. Cosmochim. Acta* 59 (17), 3469–3485.
- Gaillardet, J., Dupré, B., Allègre, C.J., Négrel, P., 1997. Chemical and physical denudation in the Amazon river basin. *Chem. Geol.* 142, 141–173.
- Gaillardet, J., Dupré, B., Allègre, C.J., 1999a. Geochemistry of

- large river suspended sediments: silicate weathering or recycling tracer? *Geochim. Cosmochim. Acta* 63 (23/24), 4037–4051.
- Gaillardet, J., Dupré, B., Louvat, P., Allègre, C.J., 1999b. Global silicate weathering and CO<sub>2</sub> consumption rates deduced from the chemistry of large rivers. *Chem. Geol.* 159, 3–30.
- Garrels, R.M., Mackenzie, F.T., 1971. *Evolutions of Sedimentary Rocks*. Norton, New York. 397 pp.
- Gibbs, R.J., 1967. The geochemistry of the Amazon river system: Part 1. The factors that control the salinity and composition and concentration of suspended solids. *Geol. Soc. Amer. Bull.*, New York 78, 1203–1232.
- Gislason, S.R., Arnorsson, S., Armannsson, H., 1996. Chemical weathering of basalt in southwest Iceland: effects of runoff, age of rocks and vegetation/glacial cover. *Am. J. Sci.* 296, 837–907.
- Goddéris, Y., François, L.M., 1995. The Cenozoic evolution of the strontium and carbon cycles: relative importance of continental erosion and mantle exchanges. *Chem. Geol.* 126, 169–190.
- Holland, D.H., 1978. *The Chemistry of Atmosphere and Oceans*. Wiley, New York. 351 pp.
- Irion, G., 1983. Clay mineralogy of the suspended load of the Amazon and of rivers in the Papua-New Guinea mainland. In: Degens, E.T., Kempe, S., Soliman, H. (Eds.), *Transport of Carbon and Minerals in Major World Rivers*, Part 2. *Mitt. Geol.-Paleontol. Inst. Univ. Hamb., SCOPE/UNEP Sond.*, vol. heft 55, pp. 483–508.
- Ludwig, W., Amiotte Suchet, P., Probst, J.L., 1999. Enhanced chemical weathering of rocks during the last glacial maximum: a sink for atmospheric CO<sub>2</sub>? *Chem. Geol.* 159, 147–161.
- Martinelli, L.A., Devol, A.H., Forsberg, B.R., Victoria, R.L., Richey, J.E., Ribeiro, M.N.G., 1989. Descarga de Sólidos Dissolvidos Totais do Rio Amazonas e seus Principais Tributários. *Geochim. Bras.*, Rio de Janeiro 3 (2), 141–148.
- Martinelli, L.A., Victoria, R.L., Dematte, J.L., Richey, J.E., Devol, A.H., 1993. Chemical and mineral composition of Amazon river floodplain sediments, Brazil. *Appl. Geochem.*, Oxford 8, 391–402.
- Meybeck, M., 1979. Concentrations des Eaux Fluviales en Éléments Majeurs et Apports en Solutions aux Océans. *Rev. Géol. Dyn. Géogr. Phys.* 21, 215–246.
- Meybeck, M., 1987. Global geochemical weathering of surficial rocks estimated from river dissolved loads. *Am. J. Sci.* 287, 401–428.
- Millot, R., Gaillardet, J., Dupré, B., Allègre, C.J., 2002. The global control of silicate weathering rates and the coupling with physical erosion: new insights from rivers of the Canadian Shield. *Earth Planet. Sci. Lett.* 196, 83–98.
- Mortatti, J., 1995. *Erosão na Amazônia: Processos, Modelos e Balanço*. Tese de Livre-Docência, Escola Superior de Agricultura Luiz de Queiroz, Universidade de São Paulo. 150 pp.
- Mortatti, J., Victoria, R.L., Tardy, Y., 1997. Balanço de Alteração e Erosão Química na Bacia Amazônica. *Geochim. Bras.* 11 (1), 2–13.
- Négre, P., Allègre, C.J., Dupré, B., Lewin, E., 1993. Erosion sources determined by inversion of major and trace element ratios in river water: the Congo basin case. *Earth Planet. Sci. Lett.* 120, 59–76.
- Nkounkou, R.R., Probst, J.L., 1987. Hydrology and geochemistry of the Congo river system. *Mitt. Geol.-Paleontol. Inst. Univ. Hamb., SCOPE/UNEP* 64, 483–508.
- Pedro, G., 1966. *Essai sur la Caractérisation Géochimique des Différents Processus Zonaux Résultant de l'altération Superficielle*. C. R. Acad. Sci., Paris 262, 1828–1831.
- Probst, J.L., 1992. *Géochimie et Hydrologie de l'Érosion Continentale*. Mécanismes, Bilan Global Actuel et Fluctuations au Cours des 500 Derniers millions d'années. *Sci. Géol. Mem.* 94 (Strasbourg), 161 pp.
- Probst, J.L., Mortatti, J., Tardy, Y., 1994. Carbon river fluxes and global weathering CO<sub>2</sub> consumption in the Congo and Amazon river basins. *Appl. Geochem.*, Oxford 9, 1–13.
- Probst, J.L., Ludwig, W., Amiotte Suchet, P., 1997. Global modeling of CO<sub>2</sub> uptake by continental erosion and of carbon river transport to the oceans. *Sci. Geol., Bull.*, Strasbourg 50 (1–4), 131–156.
- Raymo, M.E., Ruddiman, W.F., 1992. Tectonic forcing of late Cenozoic climate. *Nature* 359, 117–122.
- Richey, J.E., Salati, E., 1985. Biochemistry of the Amazon river: an update. *Mitt. Geol.-Paleontol. Inst. Univ. Hamb., SCOPE/UNEP Sonderband* 58, 245–257.
- Richey, J.E., Meade, R.H., Salati, E., Devol, A.H., Nordin, C.F., Santos, U.M., 1986. Water discharge and suspended sediment concentrations in the Amazon river. *Water Resour. Res.*, Washington 22 (5), 756–764.
- Richey, J.E., Mertes, L.A.K., Dunne, T., Victoria, R.L., Forsberg, B.R., Tancredi, A.C.N.S., Oliveira, E., 1989. Sources and routing of the Amazon river flood wave. *Glob. Biogeochem. Cycles*, Washington 3 (3), 191–204.
- Richey, J.E., Hedges, J.I., Devol, A.H., Quay, P.D., Victoria, R.L., Martinelli, L.A., Forsberg, B.R., 1990. Biogeochemistry of carbon in the Amazon river. *Limnol. Oceanogr.*, Grafton 35 (2), 352–371.
- Richey, J.E., Victoria, R.L., Salati, E., Forsberg, B.R., 1991. The biogeochemistry of a major river system: the Amazon case study. In: Degens, E.T., et al. (Eds.), *Biogeochemistry of Major World Rivers*. SCOPE, vol. 42. Wiley, New York, pp. 57–74.
- Salati, E., 1985. The climatology and hydrology of Amazonia. In: Prance, G.T., Lovejoy, T.E. (Eds.), *Amazônia*. IUCN/Pergamon, Oxford, pp. 18–48.
- Stallard, R.F., 1980. Major element geochemistry of the Amazon river system. PhD thesis, MIT-WHOI Joint Program in Oceanography, Cambridge, MA. 362 pp.
- Stallard, R.F., Edmond, J.M., 1981. Geochemistry of the Amazon: 1. Precipitation chemistry and the marine contribution to dissolved load at the time of peak discharge. *J. Geophys. Res.*, Washington 86, 9844–9858.
- Stallard, R.F., Edmond, J.M., 1983. Geochemistry of the Amazon basin: 2. The influence of the geology and weathering environment on the dissolved load. *J. Geophys. Res.*, Washington 88, 9671–9688.
- Tardy, Y., 1968. Une Méthode de Détermination des Types D'altération Actuels par L'étude des Eaux en Pays Granitiques et Gneissiques. C. R. Acad. Sci., Ser. D, Paris 267, 579–582.
- Tardy, Y., 1969. *Géochimie des Altérations*. Étude des Arènes et des Eaux de Quelques Massifs Cristallins d'Europe et d'Afrique. *Mém. Serv. Carte Géol. Alsace-Lorraine* 31 (199 pp.).

- Tardy, Y., 1971. Characterization of the principal weathering types by the geochemistry of waters from some European and African crystalline massifs. *Chem. Geol.* 7, 253–271.
- Tardy, Y., 1986. *Le Cycle de L'eau: Climats, Paléoclimats et Géochimie Globale* Masson, Paris. 338 pp.
- Tardy, Y., Mortatti, J., Victoria, R., Martinelli, L., Ribeiro, A., Cerri, C., Piccolo, M., Leite de Moraes, J., Probst, J.L., Andreux, F., Volkoff, B., 1993a. Hydroclimatology and biogeochemistry of the Amazon: Part I. Erosion. *Chem. Geol.* 107, 333–336.
- Tardy, Y., Mortatti, J., Victoria, R., Martinelli, L., Ribeiro, A., Cerri, C., Piccolo M., Leite de Moraes, J., Probst, J.L., Andreux, F., Volkoff, B., 1993b. Hydroclimatology and biogeochemistry of the Amazon: Part II. Geochemical cycles. *Chem. Geol.* 107, 411–414.
- Walker, J.C.G., Hays, P.B., Kasting, J.F., 1981. A negative feedback mechanism for the longterm stabilization of the earth's surface temperature. *J. Geophys. Res.* 86, 9776–9782.
- Wallmann, K., 2001. Controls on the cretaceous and cenozoic evolution of seawater composition, atmospheric CO<sub>2</sub> and climate. *Geochim. Cosmochim. Acta* 65, 3005–3025.
- Wei-Bin, G., 1985. Hydrochemistry of the Yangtze river basin. In: Degens, E.T., Kempe, S., Herrera, R. (Eds.), *Transport of Carbon and Minerals in Major World Rivers, Part 3*. Mitt. Geol.-Paleontol. Inst. Univ. Hamb., SCOPE/UNEP Sonderb., vol. 58, pp. 539–557.
- White, A.F., Blum, A.E., 1995. Effects of climate on chemical weathering in watersheds. *Geochim. Cosmochim. Acta* 59 (9), 1729–1747.